



Published in final edited form as:

Dev Dyn. 2012 March ; 241(3): 534–544. doi:10.1002/dvdy.23727.

Optical Coherence Tomography Captures Rapid Hemodynamic Responses to Acute Hypoxia in the Cardiovascular System of Early Embryos

Shi Gu¹, Michael W. Jenkins¹, Lindsay M. Peterson¹, Yong-Qiu Doughman², Andrew M. Rollins¹, and Michiko Watanabe²

¹Department of Biomedical Engineering, School of Medicine, Case Western Reserve University, OH 44106

²Department of Pediatrics, School of Medicine, Case Western Reserve University, OH 44106

Abstract

Background—The trajectory to heart defects may start in tubular and looping heart stages when detailed analysis of form and function is difficult by currently available methods. We used a novel method, Doppler optical coherence tomography (OCT), to follow changes in cardiovascular function in quail embryos during acute hypoxic stress. Chronic fetal hypoxia is a known risk factor for congenital heart diseases (CHDs). Decreased fetal heart rates during maternal obstructive sleep apnea suggest that studying fetal heart responses under acute hypoxia is warranted.

Results—We captured responses to hypoxia at the critical looping heart stages. Doppler OCT revealed detailed vitelline arterial pulsed Doppler waveforms. Embryos tolerated 1 hour of hypoxia (5%, 10%, or 15% O₂), but exhibited changes including decreased systolic and increased diastolic duration in 5 minutes. After 5 minutes, slower heart rates, arrhythmic events and an increase in retrograde blood flow were observed. These changes suggested slower filling of the heart, which was confirmed by 4-D Doppler imaging of the heart itself.

Conclusions—Doppler OCT is well suited for rapid non-invasive screening for functional changes in avian embryos under near physiological conditions. Analysis of the accessible vitelline artery sensitively reflected changes in heart function and can be used for rapid screening. Acute hypoxia caused rapid hemodynamic changes in looping hearts and may be a concern for increased CHD risk.

Keywords

Hypoxia; Congenital heart defects; cardiogenesis; Doppler; OCT

Introduction

Congenital heart disease (CHD), the malformation of the heart during development, is one of the most common forms of birth defects (Writing Group et al., 2009). Various risk factors, both genetic and environmental, contribute to the incidence of CHDs (Marelli et al., 2007; Michael et al., 2007). Biomechanical forces exerted by the blood flow have long been hypothesized to impact cardiac development and recent studies are beginning to elucidate the role of shear stress in controlling molecular and cellular processes [reviewed in (Groenendijk et al., 2007; Hierck et al., 2007)]. Gross alterations of hemodynamic properties at the critical looping stage have been shown to cause cardiac defects in various model systems (Hogers et al., 1997; Hogers et al., 1999; Hove et al., 2003; Reckova et al., 2003; Lucitti et al., 2006; Yashiro et al., 2007; Vermot et al., 2009), however, progress is hindered

by a lack of proper imaging techniques to quantitatively identify rapid functional changes in early embryos to identify the initial responses that deflect the heart into a trajectory towards CHDs. The heart at early looping stages is relatively small in size (0.5–1 mm in length and about 0.3 mm in diameter), fast contracting (2–3.5 Hz for avian embryos), fragile, and undergoing rapid and 3-dimensionally complex morphological changes. The heart beat is also very sensitive to environmental changes such as temperature (McQuinn et al., 2007; Vermot et al., 2009). This demands an imaging modality of high spatial resolution, fast sampling rate, easy setup, and minimal invasiveness, in order to capture the changes of hemodynamics in the looping heart. For practical purposes, a high throughput technology, where the time for set up, image capture, and analysis is short, would also be of value for experimental studies.

While many technologies have been applied to the study of the embryonic heart [reviewed in (Nieman and Turnbull, 2010; Tobita et al., 2010; Berrios-Otero et al., 2011)], previous acute functional assays on fetal hemodynamics were mostly performed using ultrasound pulsed-Doppler (Phoon, 2006; Spurney et al., 2006; McQuinn et al., 2007) with a typical axial resolution of 30 microns and a much more limited lateral resolution. While this is sufficient for interrogating hearts at later stages, the lack of spatial resolution and the requirement of direct acoustic contact with the sample make it less ideal for looping stage hearts. Optical coherence tomography (OCT) is a relatively new imaging technique (Huang et al., 1991; Gu et al., 2010; Walther et al., 2011), that is well suited to study hemodynamics in early embryos because of the high resolution that it can achieve (typically 10 microns) and its penetration depth (1–2mm) is well suited for the study of tiny embryos (Jenkins et al., 2011). The OCT penetration is much deeper than can be achieved using microscopy techniques and allows imaging of the entire heart *in vivo* during early cardiogenesis [reviewed in (Gu et al., 2010)]. Furthermore, this method requires no contact and is non-destructive, enabling observations of fragile avian embryos *in vivo* and under physiological conditions (Jenkins et al., 2010; Jenkins et al., 2011). Recent development in frequency-domain OCT and image-based retrospective gating (Garghesha et al., 2009) shed new light on the contraction dynamics of the early tubular heart (Jenkins et al., 2007), and also enabled rapidly collection of 4-D images of the beating heart to make direct hemodynamic measurements (shear stress, cardiac output, and stroke volume) (Jenkins et al., 2010).

Here, we show that when operating in the M-mode (similar to Doppler ultrasound imaging), Doppler OCT can generate pulsed Doppler waveforms at high temporal and spatial resolutions at the vitelline vessels, enabling rapid phenotypic screening of hemodynamic changes under various perturbation conditions. Because the vitelline vessel flow dynamics reflect the cardiac dynamics, this method of analyzing the morphologically simpler vitelline vessel can be used in screening for alterations of cardiac function to identify embryos that can then be subjected to the more time-consuming analysis of the beating heart itself.

To demonstrate the utility of this imaging technology, we choose hypoxia, a well-documented perturbation, for our current study. Under certain conditions, an insufficient oxygen supply (hypoxia) can occur *in utero*, which could lead to cardiac malformation (Webster and Abela, 2007; Patterson and Zhang, 2010). Conditions leading to hypoxia-related CHDs in humans include placental insufficiency (Thornburg et al., 2010), smoking (Hafström et al., 2005; Feng et al., 2010), chemical exposure (Steeg and Woolf, 1979; Arbeille et al., 1997), and extreme high altitude (Chen et al., 2009). Recent studies indicate that altered hemodynamics can also lead to CHDs (Rychter Z, 1981; Hogers et al., 1997; Forouhar et al., 2006; Culver and Dickinson, 2010), suggesting that hypoxia can exert its effects on heart development through altered hemodynamics and potentially mechanotransduction pathways. Long-term exposure of avian embryos to severe hypoxia can decrease heart rates (Mortola et al., 2010), although a decrease to 15% oxygen did not

significantly alter the embryonic heart rate (Sharma et al., 2006; Mortola et al., 2010). A similar decrease of fetal heart rate was also observed in a murine model (Furukawa et al., 2007). CHDs have been reported after prolonged hypoxic exposure (Ghatpande et al., 2008; Tintu et al., 2009; Wikenheiser et al., 2009). However, most of these experiments expose chick embryos to prolonged periods of hypoxia, and hemodynamic responses within the first hour are generally not measured. On the other hand, acute hypoxia in human pregnancy can arise with conditions such as obstructive sleep apnea (OSA) of the mother, during which slower fetal heart rates were reported (Roush and Bell, 2004; Domingo et al., 2006). Whether these acute events increase the risk for CHDs is still open for debate (Sahin et al., 2008; Ayrim et al., 2011). We decided to measure acute hemodynamic responses to various degrees of hypoxia using the avian embryo as our model system to validate our OCT imaging protocols for rapid screening of phenotypes. In the process we hoped to increase our understanding of how embryos respond to acute hypoxia with the enhanced spatial and temporal resolutions associated with OCT technology.

Results

Acute hypoxic exposure does not reduce embryo survivability

Stage 17 (Hamburger and Hamilton, 1992) quail embryos in shell-less culture were exposed to hypoxia for 1 hour, and then switched to ambient air (21% oxygen) for an additional 48 hours. The number of surviving embryos was recorded for the next 48 hours and analyzed with the Kaplan-Meier model (Kaplan and Meier, 1958) (Fig 1). Under all three hypoxic conditions, more than 80–90% of the embryos survived to the end of the 48-hour observation period and no statistically significant changes in mortality were detected. However, for the first 24 hours post exposure, there was a significant increase of mortality for embryos exposed to 5% oxygen (from 0% to 20%). This increase of mortality was limited only to the first 24 hours, and there was no additional risk for the next 24-hour period. Our explanation is that some embryos (about 15%) might be weaker and 5% oxygen merely accelerates the process of their dying; and for those embryos that were otherwise healthy, there was no additional risk associated with acute 1-hour hypoxia. Our result indicated that quail embryos in shell-less culture tolerated acute hypoxia very well without a significant increase in mortality, and the hemodynamic measurements obtained within one hour could still be considered to be under physiological conditions. We also performed experiments in which embryos were exposed to hypoxic conditions for longer times. Embryos exposed to 5% oxygen for longer than 1 hour exhibited a much stronger adverse effect with none of the embryos surviving for more than 24 hours of hypoxia exposure. On the other hand, embryos exposed to 10% or 15% oxygen survive normally under prolonged exposure up to 48 hours (data not shown).

Hemodynamics are significantly altered during the 1-hour hypoxic exposure

At stage 17 of development, quail embryos were prepared in shell-less culture and the left vitelline vessels (left omphalomesenteric artery or LOMA, shown in Figure 2A) of the developing quail embryos was located under the real-time OCT display. Operating in B-scan mode (2-D scanning mode), both the artery and vein were readily identified by OCT with the artery commonly lying deeper (Fig 2B). After switching to the M-mode (1-D data acquisition over time), images were collected at the midline of the artery (dotted line in Fig 2B), and the Doppler shift was calculated and displayed (Fig 2C). This M-mode colored Doppler display showed pulsatile blood flow patterns typical for arteries, with the red color indicating forward blood flow and the blue color indicating retrograde blood flow (Fig 2C). A seven-pixel segment was chosen at the center of the colored Doppler signal (dotted line in Fig 2C) and the pulsed Doppler waveform was computed and displayed (Fig 2D).

The same measurements were also made when the same embryos were exposed to air with reduced oxygen. When compared to the waveforms prior to the exposure, significant changes of the shape of the waveforms were detected as early as 5 minutes after the start of hypoxic exposure (Fig 3A and 3B).

We first measured well-established indices such as the pulsatility index (PI) and the resistance index (RI). These indices developed in the 1970's are widely used in Doppler ultrasound (Gosling et al., 1971; Planiol et al., 1974). They offer an overall measure of the blood flow characteristics in the arteries or heart using a single value which is not sensitive to the absolute blood flow velocity and can be easily obtained (Thompson et al., 1988). From the pulsed Doppler waveform, both indices can be easily calculated with high reproducibility from one heart beat cycle to another. Our results showed that while RI showed no significant differences, the PI of embryos exposed to either 10% or 5% oxygen is significantly increased as early as 5 minutes from the start of the exposure to hypoxic conditions (Fig 3A and 3B). In addition, some other changes were also detected. The heart rate of the embryos gradually decreased during the 1-hour exposure (Fig 3C), and in certain cases when the embryos were exposed to 5% or 10% oxygen, we also observed missing beats in a subset of the embryos (Fig 3D). Although a small number of embryos exposed to 10% oxygen were occasionally arrhythmic, prolonged arrhythmias were only observed under the most severe hypoxic condition (5% oxygen) and the embryos would likely perish shortly after persistent arrhythmia, which might explain the increase of embryo mortality during the first 24-hour period post exposure. In addition, we also observed a slight increase in retrograde blood flow in approximately 50% of the embryos exposed to 10% or 5% oxygen (Fig 3B), but this increase was not consistently observed under 15% oxygen.

Hypoxia slows down the fetal heart rate

We performed quantitative analysis on the pulsed Doppler waveforms obtained from embryos exposed to either 15%, 10%, or 5% oxygen ($n = 6$ for each group). We excluded embryos that exhibited arrhythmia during the imaging session. The first parameter measured was the heart rate (Figure 3C). By stage 17, quail embryos have a stable heart rate at about 200–220 beats per minute with no significant increase with developmental stages until stage 24 (Pearson et al., 1998). This enabled us to directly compare the heart rate before and after the hypoxic exposure even as the embryo continued to develop during the course of the experiment. Our result confirmed that stage 17 quail embryos had an average heart rate of 210 beats per minute (Figure 3C, 0 minute time point). Although a mild hypoxic exposure (15% oxygen) had no significant influence on the heart rate, both 10% and 5% oxygen exposure significantly lowered the heart rate. The changes were correlated with the length and severity of the hypoxic exposure. That is, the longer the exposure, the slower the heart rate; the more severe the hypoxia, the slower the heart rate. For example, at 5% oxygen the heart rate dropped from 210 beats per minute to about 150 beats per minute after only 25 minutes of exposure. However, these changes were mostly temporary. After the 1-hour hypoxic exposure, once the air was replaced with an ambient oxygen concentration of 21%, the heart rate gradually rose to normal levels (data not shown). The decrease of heart rate under hypoxia is consistent with previous findings under slightly different exposure protocols (Sharma et al., 2006; Mortola et al., 2010).

Since a slower heart rate indicates changes in the duration of different phases of the cardiac cycle, we measured the average systolic and diastolic time (shown in Fig 3A and 3B). As expected, the mild 15% oxygen exposure caused no changes in either phase (Fig 4A and 4B). The more severe hypoxic exposures, on the other hand, affected the phases in a complicated manner. The systolic time showed an initial decrease from 100 msec to 90 msec; it recovered to the normal levels with 10% oxygen exposure, but continued to increase to 130 msec with 5% oxygen exposure (Fig 4A). The diastolic time showed a rapid increase

at 5% and 10% oxygen (after only 5 minutes), with a much more dramatic increase under 5% oxygen exposure (from 200 msec to 300 msec, Fig 4B). Statistically, there was no further increase with longer exposure (Fig 4B). The increased duration of systole and diastole can explain the decreased heart rate. The diastolic phase was the more dominant factor because its increase was much more dramatic. This suggested that the heart spends a longer time filling, but once it is fully filled it has no major difficulties and therefore takes no extra time to pump the blood out to the arteries.

Doppler waveforms reveal other hemodynamic changes under hypoxia

During the analysis, we also consistently observed the small “shoulder” on the right side of the main forward flow peak. This shoulder has been observed in some occasions with Doppler ultrasound (Spyridopoulos et al., 2010) but has not been studied extensively due to the poor temporal resolution and noisy nature of Doppler ultrasound signals. In addition, the regions selected for analysis in M-mode Doppler ultrasound is generally large, and the heterogeneity of the velocity profile within the selected region often obscures this very subtle transition. In general, users of Doppler ultrasound utilized another index, A/B ratio, which can be obtained more consistently regardless of data quality (Stuart et al., 1980; Thompson et al., 1988). A/B ratio is the ratio of peak systolic flow and end-diastolic flow, which is a measurement of systolic/diastolic ratio (also referred to as S/D ratio). However, in our case, A/B ratio is technically meaningless due to the persistent retrograde flow at the end of diastole, rendering this ratio negative and unable to reflect the ratio of systolic/diastolic. However, we reliably observed the small secondary flow peak with distinct boundaries (Figure 2D, 3A, and 3B) because the Doppler M-mode measurement comes from a much more precise location and the velocity profile within is more uniform. Accurate measurements could therefore be made of its maximal flow. As a result, we could calculate the ratio of the secondary peak over the primary peak and obtain a systolic/diastolic ratio that is a more direct measure than the conventional A/B ratio. When we measured the relative height of this “shoulder” against the maximal forward flow, there was a significant decrease after 25 minutes of exposure under the more severe 10% and 5% oxygen concentration. The mild hypoxia (15% oxygen) showed no statistically significant changes. Since the systolic time is not significantly affected by hypoxic exposures, the observed decrease of this ratio suggests a less vigorous blood filling of the heart during diastole. This is consistent with our earlier observation of increased diastolic time, because it takes longer to fully fill the heart chamber before the next contraction can start.

4-D Doppler profiles in the beating heart under hypoxic conditions—From the pulsed Doppler waveforms obtained from the vitelline arteries, we deduced what might be happening inside of the heart. Based on our analyses, we hypothesized that the heart must have a prolonged phase during blood filling. To directly test this hypothesis, we performed 4-D OCT imaging on a stage 14 quail heart before and after 1-hour of 5% oxygen exposure (see movie in supplemental data).

To perform the experiment, we took an approach that is described in more detail in our earlier publications (Jenkins et al., 2010). As it currently takes a much longer time to collect and process the whole 4-D dataset from the 3-dimensionally complex looped heart than from the tubular vitelline artery, we limited our analysis to only one experimental condition (stage 14 embryo, 5% oxygen, 1-hour exposure time). We could, however, use the same 4-D dataset to make more advanced measurements (e.g. shear stress, or contractile wave propagation velocity) in the future. We chose not to image stage 17 quail embryos for practical reasons. The OCT imaging system has limited penetration depth and allowed a much better view at stage 14 than at stage 17. Furthermore, the response to hypoxia of the stage 14 embryo proved to be similar to the stage 17 embryo. The blood flow at both the

inflow and outflow portion of the heart is easily detected by Doppler OCT, as shown in the movie, whereas the top of the heart tube shows little Doppler signal due to the incident angle of the light being nearly perpendicular to the flow direction. When the Doppler profile under hypoxia was compared to the normoxic control, the blood flow velocity at the inflow side appeared to be significantly lower. In addition, the heart appeared to “pause” at the end of the filling stage before the forward contraction began, which was predicted from our waveform analysis of a prolonged diastolic phase measured at the vitelline artery. The blood flow patterns obtained directly from the beating heart confirmed what we deduced from the observations made in the vitelline arteries with M-mode pulsed Doppler waveform analyses.

Discussion

Doppler OCT provides high resolution pulsed Doppler waveforms that can be used to measure hemodynamic parameters

During fetal cardiovascular system development, shear stress induced by blood flow has been demonstrated to play important roles (Culver and Dickinson, 2010). The traditional approach to obtain such information is to use M-mode Doppler ultrasound (Clark et al., 1986; Hu and Clark, 1989; McQuinn et al., 2007; Oosterbaan et al., 2009). However, ultrasound has limited spatial resolution which limits its usefulness during early embryonic development where the size of the heart tube or vessels of interest are less than 250 micrometers in diameter. Compared to Doppler ultrasound, Doppler OCT may have significant advantages when imaging early embryos because of its high spatial and temporal resolution. The typical waveform obtained with OCT clearly displays features that are difficult to detect in ultrasound waveforms. For example, we reliably demonstrated the small retrograde flow leading to the upstroke of each heart beat (Fig 2D), which is harder to identify with ultrasound. We also demonstrated a clear “shoulder” wave following the systolic contraction (Fig 2D), which is also harder to define with ultrasound. With pulsed ultrasound, the signal is derived from a much larger region of interest (ROI) compared to Doppler OCT. When a larger region is selected, the region often encompasses extraneous tissues (e.g. vessel wall) that can increase the noise. The blood flow inside a blood vessel can be viewed as having a parabolic profile with the velocity at the center being highest, and that near the vessel wall being the lowest. A larger ROI leads to a wide distribution in velocities, and the result is a wide distribution on the pulsed Doppler waveforms. Also, our 4-D movie demonstrates that the pulsed waveforms vary greatly over a small region (inflow versus outflow) which means that the larger ROI in pulsed Doppler ultrasound may lead to the combination of several unique waveforms into one composite trace. A smaller region of interest can be selected for Doppler OCT, thereby minimizing noise in the signal from the overlapping signals and extraneous tissue. Also, Doppler OCT and ultrasound signals are generally noisy and require averaging to produce reliable signals. The increased spatial and temporal (8 microseconds/A-scan) resolution of OCT can be employed for signal averaging to increase the signal to noise ratio. In general, we have seen a much more clearly defined trace in the waveforms than can be obtained with ultrasound (Fig 2D), which enabled us to detect more subtle features such as the “shoulder” and the retrograde blood flows. However, OCT has less penetration depth than ultrasound, usually about 1–2 millimeters. This might limit its use when studying late-stage embryos or adult animals. Ideally, OCT would be used for early-stage observations and ultrasound for late-stage observations.

Here, we demonstrated that by using Doppler OCT, we can generate pulsed Doppler waveforms from locations such as the vitelline arteries in an early avian embryo. These waveforms can be analyzed to offer informative details about the functions of the heart. This approach has several advantages, including an easy setup, high spatial and temporal resolutions, and rapid analysis of data. Combined with a culture chamber to closely control environmental conditions, this method offers a non-invasive means to perform longitudinal

studies. This is particularly important for developmental biology studies, due to high variances in stage within incubation days and within a stage among individual embryos especially at early stages. A longitudinal study offers internal controls before and after any interventions or treatments, thus reducing the numbers of specimens needed to perform experiments. Using M-mode Doppler OCT, an observation can be made in only a few minutes, which is also essential for short-term experiments such as in the study of acute responses to hypoxic exposure. For example, after 5 minutes of exposure to hypoxia, embryos initially responded by transiently shortening systolic time. This could help to explain the initial increase of the heart rate observed by Sedmera et al in their explanted heart model (Sedmera et al., 2002). This illustrates that the looping heart responds to stimuli very quickly, therefore it is important to have an easy setup and ability to record data quickly. In the future, we plan to modify our imaging protocol to allow continuous data recording. This will also allow studies related to intermittent arrhythmias. Our current imaging protocol can only capture arrhythmia events if they happen to fall inside our short recording time windows.

Pulsed Doppler waveform analysis is suitable for initial screens—A Doppler signal is only sensitive in the direction of the incident beam, and the flow information perpendicular to the beam direction is lost during the measurement. To obtain the actual flow velocity, the angle between the beam and the flow direction has to be measured (Wang et al., 2007; Jenkins et al., 2010). On the other hand, the pulsed Doppler waveform ignores such corrections and displays its result as a normalized flow pattern versus time. There are several advantages; (1) the shape of the waveform is not affected by the angle between the beam and the flow, and (2) the region of interest does not have to be in the center of the vessel. As a result, we can operate in M-mode with a single line-scan passing through the artery. Therefore, as an initial screen, pulsed Doppler OCT in M-mode is much simpler to set up and the benefit in temporal resolution outweighs the loss (cannot obtain absolute velocity information).

After analyzing the pulsed Doppler waveforms obtained from the vitelline vessels, we inferred that the embryonic heart had a prolonged filling stage under hypoxia. This was confirmed by 4-D Doppler imaging performed directly on the embryonic heart that showed weaker filling and a pause at the end of diastole. Therefore, we conclude that pulsed Doppler waveform analyses performed at the vitelline vessels can offer a quick and easy preview of what might be happening in the heart. It is well suited as a tool for initial screening for functional changes before more elaborate techniques are used to undertake the more complex and time-consuming cardiac function analyses in the heart. In this paper, we used 4-D Doppler imaging only to visually verify the change of cardiac function; however, precise measurements (e.g. wall shear stress, myocardial strain and stretch) can be obtained based on the same dataset in the future, and these more advanced measurements can greatly contribute to our understanding of biomechanical forces within the heart and their roles to cardiac development.

Acute hypoxia can rapidly change hemodynamics of the embryo—Previous studies on hypoxia were mostly focused on long-term exposures (Arbeille et al., 1997; Hafström et al., 2005; Naňka et al., 2006; Sharma et al., 2006; Webster and Abela, 2007; Ghatpande et al., 2008; Nanka et al., 2008; Tintu et al., 2009; Wikenheiser et al., 2009; Patterson and Zhang, 2010), where the transcriptional activity of HIF-1 and HIF-2 are likely to play a role in the outcome (Compennolle et al., 2003; Webster and Abela, 2007; Xu et al., 2007; Wikenheiser et al., 2009; Patterson and Zhang, 2010). Although there were reports of decreased heart rate, it was not possible to determine whether this was due to the roles of HIF or other factors because of the length of hypoxia exposure and the time when the function was assessed (Mortola et al., 2010). We have presented compelling evidence that

some aspects of hemodynamics can be altered by hypoxia as early as 5 minutes, which is too rapid to be accounted for by HIF-mediated transcriptional regulation. We do not yet know the mechanisms of such alterations; although it seems reasonable to hypothesize that hypoxia may change the energy balance of the cell (Budinger et al., 1996) and cause changes in cardiac contraction or conduction. Hemodynamic changes have been proposed as a mechanism for CHDs (Culver and Dickinson, 2010), however, we do not yet know if the changes associated with acute hypoxia can produce developmental defects. Our survival analyses indicated no significant increase in mortality with the exception of exposure to 5% oxygen concentration. Even under the most severe condition, hypoxia appears to only shift the time of death for the weakest embryos, as 15–20% of them died during the first 24 hours instead of the second 24 hours period. Temporary hypoxia in humans can result from conditions such as obstructive sleep apnea where fetal heart rate deceleration has been reported in such cases (Roush and Bell, 2004; Sahin et al., 2008). It is important to understand the link between hypoxia, hemodynamics, and CHDs, to properly assess the risks to the fetus in these situations. Our results suggested that such intermittent hemodynamic changes may not result in cardiac defects in healthy individuals; however, if combined with other risk factor for CHDs, they may still have significant impact on fetal outcome. Further experiments are clearly warranted to fully elucidate those connections.

Even in prolonged hypoxic exposure, we can conclude that HIF-mediated transcriptional events are not the only pathways involved. Hypoxia itself can alter the blood flow pattern before HIF-1 or HIF-2 can perform their gene regulatory functions. Although HIF activation may still contribute to the process, including a potential adaptive response to hypoxia, non-HIF related targets might need to be considered for therapy and prevention. It is known that shear forces or cyclic strains can also alter gene expression (Awolesi et al., 1994; Pearce et al., 1996; Azuma et al., 2000; Dekker et al., 2002), some of which are shown to be important in cardiovascular development, such as in the activation and upregulation of eNOS (Kumar et al., 2008), klf2 (Lee et al., 2006), and p-ERK (Liberatore and Yutzey, 2004; Krenz et al., 2005). ERK phosphorylation happens within 5 minutes of altered shear stress (Pearce et al., 1996; Azuma et al., 2000), and therefore might mediate effects seen in acute hypoxia. Thus the regulatory mechanisms that drive the responses of the cell or tissue to adapt to hypoxia likely include both HIF-dependent and HIF-independent mechanisms. The HIF-independent mechanisms could include rapid responses of the heart that alter function that in turn can alter gene expression through mechanotransduction pathways.

In conclusion, Doppler OCT of the accessible vitelline artery sensitively reflected subtle changes in function of the looping avian heart. This method could be useful as a rapid screen to identify embryos with functional changes in cardiac function. Using this method we found that acute hypoxia caused rapid hemodynamic changes including an increase in retrograde flow in looping hearts that may be a concern for increased CHD risk.

Experimental Procedures

Quail egg incubation and shell-less culture

Fertilized quail eggs (*Coturnix coturnix communis*; Boyd's Bird Company, Inc., Pullman, WA) were incubated in a humidified, forced draft incubator (G.Q.F. Manufacturing Co., Savannah, GA) at 38°C for 48 hours. Each egg was removed from the incubator, the shell removed and the content of the egg was placed in a sterilized 35 mm Petri dish (Dunn, 1974). This shell-less culture was placed in a humidified tissue culture incubator (New Brunswick Scientific, Edison, NJ) at 38°C until imaging.

OCT imaging setup and imaging protocol

The OCT imaging system used in this study was a custom-built swept source OCT system, employing a buffered Fourier Domain Mode Locked (FDML) laser (Huber et al., 2006a; Huber et al., 2006b), which operates at a 117 kHz line rate. The axial resolution of the system was 8 μm in tissue and the lateral resolution was $\sim 10 \mu\text{m}$ (Jenkins et al., 2011). At stage 17 of development, quail embryos were prepared in a shell-less culture and the left side of the vitelline vessels was imaged with the OCT system as described in the results section (Figure 2). The real-time B-scan was scanned at 500 lines per image (Fig 2B). For the Doppler measurements, the OCT system was operated at slower line rate (29 kHz) to improve sensitivity to Doppler shift caused by blood flow (Fig 2C).

Pulsed Doppler waveform analysis

Pulsed Doppler waveforms are generated using Matlab (MathWorks, Massachusetts), and both heart rate and common indices such as pulsatility index (PI) (Gosling et al., 1971) and resistance index (RI) (Planiol et al., 1974) were calculated with Matlab. PI and RI are defined by

$$PI = \frac{Max - Min}{Avg}, \quad RI = \frac{Max - Min}{Max}$$

where *Max* is the maximal Doppler shift, *Min* is the minimal Doppler shift, and *Avg* is the time-averaged Doppler shift.

We also measured other parameters that are defined as following. Relative “shoulder” height is defined as the ratio of secondary peak height (*h2*) to the main peak height (*h1* or *Max*) (Fig 2D). We next define time point *t2* as the start time of the secondary peak; *t1* is the corresponding time point during the upstroke with the same Doppler shift as *t2*. The time span from *t1* to *t2* is defined as systolic time, and the rest of the heart cycle is defined as diastolic time (Fig 2D).

4-D Doppler OCT of the embryonic heart

Each embryo in shell-less culture was placed under the OCT system at about 50–53 hours of development. The developing heart imaged at 70 parallel slices, which were parallel to the body axis and spaced every 20 μm . At each slice position, 70 B-scan images (1000 lines per image, 1.5 μm between each line) were taken before the scanner moved to the next slice position. After all the data were collected, an image-based retrospective gating algorithm (Garghesha et al., 2009) was used to reconstruct the beating heart in 3D. The Doppler shift was calculated and the phase was unwrapped (Goldstein et al., 1988) and displayed as an overlay to the structure image using Matlab (Jenkins et al., 2010).

Imaging chamber setup and hypoxic exposure protocol

Quail embryo cultures were placed in a hypoxia chamber with a transparent lid. The oxygen concentration in the chamber was monitored by a gas oxygen controller (*ProOx360*, *BioSpherix*, *Lacona, NY*). The hypoxia chamber was housed in a humidified culture incubator, where the temperature and humidity were controlled to maintain the developing embryo under physiological conditions (Jenkins et al., 2011). During hypoxic exposure, the gas oxygen controller controlled the slow release of nitrogen gas into the hypoxia chamber until the desired oxygen concentration was reached. For the acute hypoxic exposure, the embryos were exposed to decreasing oxygen concentration at 15%, 10% or 5% (regular ambient air contains 21% oxygen) for 1 hour then returned to normoxia. During the 1-hour

exposure, pulsed Doppler waveforms were recorded in the vitelline artery at 5, 15, 25, 35, 45, and 60-minute time points, and compared to those measured prior to the hypoxic exposure (0 minute, and 21% oxygen concentration).

Survival analysis after short-term hypoxic exposure

After incubation for 48 hours, shell-less cultures were made as described earlier and placed in the humidified culture incubator and cultured for another 24 hours at 38°C. Afterwards, the surviving embryos (usually >90% survival rate) were exposed to either hypoxic conditions (15%, 10%, or 5% oxygen) for 1 hour, or control conditions (no change in oxygen concentration). After one hour of hypoxic exposure, the embryo's environment was changed back to a normal oxygen concentration. During the next 48 hours, the survival of the cultures was recorded at 6 hours intervals. A statistical analysis was performed to identify any potential increase in mortality after 1-hour of acute hypoxic exposure.

Statistical analysis

All statistical analyses were performed with the software package SPSS (IBM Corporation, Somers, NY), and a *p*-value of 0.05 is used to establish statistical significance. The Kaplan-Meier survival analyses (Kaplan and Meier, 1958) were performed for both the short-term survival (24 hours post exposure) and long-term survival (48 hours post exposure). For the pulsed Doppler waveform analyses, one-way ANOVA was performed to identify potential significant differences, and the Tukey's *post-hoc* comparisons were performed only when significant differences existed.

Supplementary Material

Refer to Web version on PubMed Central for supplementary material.

Acknowledgments

This project was supported by grant numbers HL083048 and HL095717 (to AR & MW), and by American Recovery and Reinvestment Act (ARRA) funds through grant number R01 HL091171 (to MW) from the National Heart, Lung, and Blood Institute, National Institutes of Health. The authors want to specially thank Dr. Siting Wang for advice on the statistical analyses.

References

- Arbeille P, Maulik D, Salihagic A, Locatelli A, Lansac J, Platt LD. Effect of long-term cocaine administration to pregnant ewes on fetal hemodynamics, oxygenation, and growth. *Obstet Gynecol.* 1997; 90:795–802. [PubMed: 9351767]
- Awolesi MA, Widmann MD, Sessa WC, Sumpio BE. Cyclic strain increases endothelial nitric oxide synthase activity. *Surgery.* 1994; 116:439–444. discussion 444–435. [PubMed: 7519368]
- Ayrim A, Keskin E, Ozol D, Onaran Y, Yildirim Z, Kafali H. Influence of self-reported snoring and witnessed sleep apnea on gestational hypertension and fetal outcome in pregnancy. *Archives of Gynecology and Obstetrics.* 2011; 283:195–199. [PubMed: 20033421]
- Azuma N, Duzgun SA, Ikeda M, Kito H, Akasaka N, Sasajima T, Sumpio BE. Endothelial cell response to different mechanical forces. *Journal of Vascular Surgery.* 2000; 32:789–794. [PubMed: 11013043]
- Berrios-Otero CA, Nieman BJ, Parasoglou P, Turnbull DH. In utero phenotyping of mouse embryonic vasculature with MRI. *Magn Reson Med.* 2011
- Budinger GR, Chandel N, Shao ZH, Li CQ, Melmed A, Becker LB, Schumacker PT. Cellular energy utilization and supply during hypoxia in embryonic cardiac myocytes. *American Journal of Physiology - Lung Cellular and Molecular Physiology.* 1996; 270:L44–L53.

- Chen QH, Liu FY, Wang XQ, Qi GR, Liu PF, Jin XH, Lu L, Zhao GQ, Qi SG. A cross-sectional study of congenital heart disease among children aged from 4 to 18 years at different altitudes in Qinghai province, China. *Zhonghua Liu Xing Bing Xue Za Zhi*. 2009; 30:1248–1251. [PubMed: 20193307]
- Clark EB, Hu N, Dummett JL, Vandekieft GK, Olson C, Tomanek R. Ventricular function and morphology in chick embryo from stages 18 to 29. *American Journal of Physiology -Heart and Circulatory Physiology*. 1986; 250:H407–H413.
- Compernelle V, Brusselmans K, Franco D, Moorman A, Dewerchin M, Collen D, Carmeliet P. Cardia bifida, defective heart development and abnormal neural crest migration in embryos lacking hypoxia-inducible factor-1 α . *Cardiovascular Research*. 2003; 60:569–579. [PubMed: 14659802]
- Culver JC, Dickinson ME. The Effects of Hemodynamic Force on Embryonic Development. *Microcirculation*. 2010; 17:164–178. [PubMed: 20374481]
- Dekker RJ, van Soest S, Fontijn RD, Salamanca S, de Groot PG, VanBavel E, Pannekoek H, Horrevoets AJG. Prolonged fluid shear stress induces a distinct set of endothelial cell genes, most specifically lung Kruppel-like factor (KLF2). *Blood*. 2002; 100:1689–1698. [PubMed: 12176889]
- Domingo C, Latorre E, Mirapeix RM, Abad J. Snoring, obstructive sleep apnea syndrome, and pregnancy. *International Journal of Gynecology & Obstetrics*. 2006; 93:57–59. [PubMed: 16530765]
- Dunn BE. Technique of shell-less culture of the 72-hour avian embryo. *Poult Sci*. 1974; 53:409–412. [PubMed: 4833046]
- Feng Y, Caiping M, Li C, Can R, Feichao X, Li Z, Zhice X. Fetal and offspring arrhythmia following exposure to nicotine during pregnancy. *Journal of Applied Toxicology*. 2010; 30:53–58. [PubMed: 19728315]
- Fouhar AS, Liebling M, Hickerson A, Nasiraei-Moghaddam A, Tsai H-J, Hove JR, Fraser SE, Dickinson ME, Gharib M. The Embryonic Vertebrate Heart Tube Is a Dynamic Suction Pump. *Science*. 2006; 312:751–753. [PubMed: 16675702]
- Furukawa S, Tinney JP, Tobita K, Keller BB. Hemodynamic vulnerability to acute hypoxia in day 10.5–16.5 murine embryos. *Journal of Obstetrics and Gynaecology Research*. 2007; 33:114–127. [PubMed: 17441882]
- Gargasha M, Jenkins MW, Wilson DL, Rollins AM. High temporal resolution OCT using image-based retrospective gating. *Opt Express*. 2009; 17:10786–10799. [PubMed: 19550478]
- Ghatpande SK, Billington CJ, Rivkees SA, Wendler CC. Hypoxia induces cardiac malformations via A1 adenosine receptor activation in chicken embryos. *Birth Defects Research Part A: Clinical and Molecular Teratology*. 2008; 82:121–130.
- Goldstein RM, Zebker HA, Werner CL. Satellite radar interferometry: Two-dimensional phase unwrapping. *Radio Sci*. 1988; 23:713–720.
- Gosling RG, Dunbar G, King DH, Newman DL, Side CD, Woodcock JP, Fitzgerald DE, Keates JS, Macmillan D. The Quantitative Analysis of Occlusive Peripheral Arterial Disease By a Non-Intrusive Ultrasonic Technique. *Angiology*. 1971; 22:52–55. [PubMed: 5101050]
- Groenendijk BCW, Van der Heiden K, Hierck BP, Poelmann RE. The Role of Shear Stress on ET-1, KLF2, and NOS-3 Expression in the Developing Cardiovascular System of Chicken Embryos in a Venous Ligation Model. *Physiology*. 2007; 22:380–389. [PubMed: 18073411]
- Gu, S.; Jenkins, MW.; Watanabe, M.; Rollins, AM. High-Speed Optical Coherence Tomography Imaging of the Beating Avian Embryonic Heart. In: Wong, R.; Sharpe, J., editors. *Imaging in Developmental Biology: A Laboratory Manual*. Cold Spring Harbor Laboratory Press; 2010.
- Hafström O, Milerad J, Sandberg KL, Sundell HW. Cardiorespiratory effects of nicotine exposure during development. *Respiratory Physiology & Neurobiology*. 2005; 149:325–341. [PubMed: 15970470]
- Hamburger V, Hamilton HL. A series of normal stages in the development of the chick embryo. 1951. *Dev Dyn*. 1992; 195:231–272. [PubMed: 1304821]
- Hierck BP, van der Heiden K, DeRuiter MC, Gittenberger-de Groot AC, Poelmann RE. Fluid shear stress controls cardiovascular development. A functionomic approach. *Wien Klin Wochenschr*. 2007; 119:10–13. [PubMed: 19618590]

- Hogers B, DeRuiter MC, Gittenberger-de Groot AC, Poelmann RE. Unilateral Vitelline Vein Ligation Alters Intracardiac Blood Flow Patterns and Morphogenesis in the Chick Embryo. *Circulation Research*. 1997; 80:473–481. [PubMed: 9118477]
- Hogers B, DeRuiter MC, Gittenberger-de Groot AC, Poelmann RE. Extraembryonic venous obstructions lead to cardiovascular malformations and can be embryolethal. *Cardiovascular Research*. 1999; 41:87–99. [PubMed: 10325956]
- Hove JR, Koster RW, Forouhar AS, Acevedo-Bolton G, Fraser SE, Gharib M. Intracardiac fluid forces are an essential epigenetic factor for embryonic cardiogenesis. *Nature*. 2003; 421:172–177. [PubMed: 12520305]
- Hu N, Clark E. Hemodynamics of the stage 12 to stage 29 chick embryo. *Circulation Research*. 1989; 65:1665–1670. [PubMed: 2582595]
- Huang D, Swanson E, Lin C, Schuman J, Stinson W, Chang W, Hee M, Flotte T, Gregory K, Puliafito C, et al. Optical coherence tomography. *Science*. 1991; 254:1178–1181. [PubMed: 1957169]
- Huber R, Adler DC, Fujimoto JG. Buffered Fourier domain mode locking: unidirectional swept laser sources for optical coherence tomography imaging at 370,000 lines/s. *Opt Lett*. 2006a; 31:2975–2977. [PubMed: 17001371]
- Huber R, Wojtkowski M, Fujimoto JG. Fourier Domain Mode Locking (FDML): A new laser operating regime and applications for optical coherence tomography. *Opt Express*. 2006b; 14:3225–3237. [PubMed: 19516464]
- Jenkins MW, Adler DC, Garghesha M, Huber R, Rothenberg F, Belding J, Watanabe M, Wilson DL, Fujimoto JG, Rollins AM. Ultrahigh-speed optical coherence tomography imaging and visualization of the embryonic avian heart using a buffered Fourier Domain Mode Locked laser. *Opt Express*. 2007; 15:6251–6267. [PubMed: 19546930]
- Jenkins MW, Peterson L, Gu S, Garghesha M, Wilson DL, Watanabe M, Rollins AM. Measuring hemodynamics in the developing heart tube with four-dimensional gated Doppler optical coherence tomography. *J Biomed Opt*. 2010; 15:066022. [PubMed: 21198196]
- Jenkins MW, Watanabe M, Rollins AM. Longitudinal Imaging of Heart Development with Optical Coherence Tomography. *Selected Topics in Quantum Electronics, IEEE Journal*. 2011:1–1.
- Kaplan EL, Meier P. Nonparametric Estimation from Incomplete Observations. *Journal of the American Statistical Association*. 1958; 53:457–481.
- Krenz M, Yutzey KE, Robbins J. Noonan Syndrome Mutation Q79R in Shp2 Increases Proliferation of Valve Primordia Mesenchymal Cells via Extracellular Signal-Regulated Kinase 1/2 Signaling. *Circ Res*. 2005; 97:813–820. [PubMed: 16166557]
- Kumar SD, Yong S-K, Dheen ST, Bay B-H, Tay SS-W. Cardiac Malformations Are Associated with Altered Expression of Vascular Endothelial Growth Factor and Endothelial Nitric Oxide Synthase Genes in Embryos of Diabetic Mice. *Exp Biol Med*. 2008; 233:1421–1432.
- Lee JS, Yu Q, Shin JT, Sebzda E, Bertozzi C, Chen M, Mericko P, Stadtfeld M, Zhou D, Cheng L, Graf T, MacRae CA, Lepore JJ, Lo CW, Kahn ML. Klf2 Is an Essential Regulator of Vascular Hemodynamic Forces In Vivo. *Developmental Cell*. 2006; 11:845–857. [PubMed: 17141159]
- Liberatore CM, Yutzey KE. MAP kinase activation in avian cardiovascular development. *Developmental Dynamics*. 2004; 230:773–780. [PubMed: 15254911]
- Lucitti JL, Visconti R, Novak J, Keller BB. Increased arterial load alters aortic structural and functional properties during embryogenesis. *American Journal of Physiology - Heart and Circulatory Physiology*. 2006; 291:H1919–H1926. [PubMed: 16648183]
- Marelli AJ, Mackie AS, Ionescu-Ittu R, Rahme E, Pilote L. Congenital Heart Disease in the General Population: Changing Prevalence and Age Distribution. *Circulation*. 2007; 115:163–172. [PubMed: 17210844]
- McQuinn TC, Bratoeva M, Dealmeida A, Remond M, Thompson RP, Sedmera D. High-frequency ultrasonographic imaging of avian cardiovascular development. *Dev Dyn*. 2007; 236:3503–3513. [PubMed: 17948299]
- Michael EM, Tara LS, Denise BK, Aoy T-M. The Molecular Basis of Congenital Heart Disease. *Seminars in thoracic and cardiovascular surgery*. 2007; 19:228–237. [PubMed: 17983950]

- Mortola JP, Wills K, Trippenbach T, Al Awam K. Interactive effects of temperature and hypoxia on heart rate and oxygen consumption of the 3-day old chicken embryo. *Comparative Biochemistry and Physiology - Part A: Molecular & Integrative Physiology*. 2010; 155:301–308.
- Nanka O, Krizova P, Fikrle M, Tuma M, Blaha M, Grim M, Sedmera D. Abnormal Myocardial and Coronary Vasculature Development in Experimental Hypoxia. *The Anatomical Record: Advances in Integrative Anatomy and Evolutionary Biology*. 2008; 291:1187–1199.
- Naňka O, Valášek P, Dvořáková M, Grim M. Experimental hypoxia and embryonic angiogenesis†. *Developmental Dynamics*. 2006; 235:723–733. [PubMed: 16444736]
- Nieman BJ, Turnbull DH. Ultrasound and magnetic resonance microimaging of mouse development. *Methods Enzymol*. 2010; 476:379–400. [PubMed: 20691877]
- Oosterbaan AM, Ursem NTC, Struijk PC, Bosch JG, van der Steen AFW, Steegers EAP. Doppler flow velocity waveforms in the embryonic chicken heart at developmental stages corresponding to 5–8 weeks of human gestation. *Ultrasound in Obstetrics and Gynecology*. 2009; 33:638–644. [PubMed: 19434670]
- Patterson AJ, Zhang L. Hypoxia and fetal heart development. *Curr Mol Med*. 2010; 10:653–666. [PubMed: 20712587]
- Pearce MJ, McIntyre TM, Prescott SM, Zimmerman GA, Whatley RE. Shear Stress Activates Cytosolic Phospholipase A2(cPLA2) and MAP Kinase in Human Endothelial Cells. *Biochemical and Biophysical Research Communications*. 1996; 218:500–504. [PubMed: 8561785]
- Pearson J, Tsudzuki M, Nakane Y, Akiyama R, Tazawa H. Development of heart rate in the precocial king quail *Coturnix chinensis*. *J Exp Biol*. 1998; 201:931–941. [PubMed: 9487098]
- Phoon CK. Imaging tools for the developmental biologist: ultrasound biomicroscopy of mouse embryonic development. *Pediatr Res*. 2006; 60:14–21. [PubMed: 16690959]
- Planiol T, Pourcelot L, Itti R. Radioisotopes, ultrasonics and thermography in the diagnosis of cerebral circulatory disorders. *Rev Electroencephalogr Neurophysiol Clin*. 1974; 4:221–236. [PubMed: 4608395]
- Reckova M, Rosengarten C, deAlmeida A, Stanley CP, Wessels A, Gourdie RG, Thompson RP, Sedmera D. Hemodynamics Is a Key Epigenetic Factor in Development of the Cardiac Conduction System. *Circulation Research*. 2003; 93:77–85. [PubMed: 12775585]
- Roush SF, Bell L. Obstructive Sleep Apnea in Pregnancy. *J Am Board Fam Pract*. 2004; 17:292–294. [PubMed: 15243018]
- Rychter, ZRV. Perspectives in Cardiovascular Research, Mechanisms of Cardiac Morphogenesis and Teratogenesis. In: TP, editor. *Angio- and myoarchitecture of the heart wall under normal and experimentally changed morphogenesis*. New York: Raven Press; 1981. p. 431–452.
- Sahin FK, Koken G, Cosar E, Saylan F, Fidan F, Yilmazer M, Unlu M. Obstructive sleep apnea in pregnancy and fetal outcome. *International Journal of Gynecology & Obstetrics*. 2008; 100:141–146. [PubMed: 17976624]
- Sedmera D, Kucera P, Raddatz E. Developmental changes in cardiac recovery from anoxia-reoxygenation. *Am J Physiol Regul Integr Comp Physiol*. 2002; 283:R379–388. [PubMed: 12121851]
- Sharma SK, Lucitti JL, Nordman C, Tinney JP, Tobita K, Keller BB. Impact of hypoxia on early chick embryo growth and cardiovascular function. *Pediatr Res*. 2006; 59:116–120. [PubMed: 16327005]
- Spurney CF, Lo CW, Leatherbury L. Fetal Mouse Imaging Using Echocardiography: A Review of Current Technology. *Echocardiography*. 2006; 23:891–899. [PubMed: 17069613]
- Spyridopoulos TN, Kaziani K, Balanika AP, Kalokairinou-Motogna M, Bizimi V, Paianidi I, Baltas CS. Ultrasound as a first line screening tool for the detection of renal artery stenosis: a comprehensive review. *Med Ultrason*. 2010; 12:228–232. [PubMed: 21203601]
- Stegg CN, Woolf P. Cardiovascular malformations in the fetal alcohol syndrome. *Am Heart J*. 1979; 98:635–637. [PubMed: 158960]
- Stuart B, Drumm J, FitzGerald DE, Duignan NM. Fetal blood velocity waveforms in normal pregnancy. *Br J Obstet Gynaecol*. 1980; 87:780–785. [PubMed: 7426537]
- Thompson RS, Trudinger BJ, Cook CM. Doppler ultrasound waveform indices: A/B ratio, pulsatility index and Pourcelot ratio. *Br J Obstet Gynaecol*. 1988; 95:581–588. [PubMed: 3291936]

- Thornburg KL, O'Tierney PF, Louey S. Review: The Placenta is a Programming Agent for Cardiovascular Disease. *Placenta*. 2010; 31:S54–S59. [PubMed: 20149453]
- Tintu A, Rouwet E, Verlohren S, Brinkmann J, Ahmad S, Crispi F, van Bilsen M, Carmeliet P, Staff AC, Tjwa M, Cetin I, Gratacos E, Hernandez-Andrade E, Hofstra L, Jacobs M, Lamers WH, Morano I, Safak E, Ahmed A, le Noble F, Schwartz A. Hypoxia Induces Dilated Cardiomyopathy in the Chick Embryo: Mechanism, Intervention, and Long-Term Consequences. *PLoS ONE*. 2009; 4:e5155. [PubMed: 19357774]
- Tobita K, Liu X, Lo CW. Imaging modalities to assess structural birth defects in mutant mouse models. *Birth Defects Res C Embryo Today*. 2010; 90:176–184. [PubMed: 20860057]
- Vermot J, Forouhar AS, Liebling M, Wu D, Plummer D, Gharib M, Fraser SE. Reversing blood flows act through *klf2a* to ensure normal valvulogenesis in the developing heart. *PLoS Biol*. 2009; 7:e1000246. [PubMed: 19924233]
- Walther J, Gaertner M, Cimalla P, Burkhardt A, Kirsten L, Meissner S, Koch E. Optical coherence tomography in biomedical research. *Anal Bioanal Chem*. 2011; 400:2721–2743. [PubMed: 21562739]
- Wang Y, Bower BA, Izatt JA, Tan O, Huang D. In vivo total retinal blood flow measurement by Fourier domain Doppler optical coherence tomography. *Journal of Biomedical Optics*. 2007; 12:041215–041218. [PubMed: 17867804]
- Webster WS, Abela D. The effect of hypoxia in development. *Birth Defects Research Part C: Embryo Today: Reviews*. 2007; 81:215–228.
- Wikenheiser J, Wolfram JA, Gargasha M, Yang K, Karunamuni G, Wilson DL, Semenza GL, Agani F, Fisher SA, Ward N, Watanabe M. Altered hypoxia-inducible factor-1 alpha expression levels correlate with coronary vessel anomalies. *Developmental Dynamics*. 2009; 238:2688–2700. [PubMed: 19777592]
- Lloyd-Jones D, Adams R, Carnethon M, De Simone G, Ferguson TB, Flegal K, Ford E, Furie K, Go A, Greenlund K, Haase N, Hailpern S, Ho M, Howard V, Kissela B, Kittner S, Lackland D, Lisabeth L, Marelli A, McDermott M, Meigs J, Mozaffarian D, Nichol G, O'Donnell C, Roger V, Rosamond W, Sacco R, Sorlie P, Stafford R, Steinberger J, Thom T, Wasserthiel-Smoller S, Wong N, Wylie-Rosett J, Hong Y. Writing Group M. for the American Heart Association Statistics C, Stroke Statistics S. Heart Disease and Stroke Statistics--2009 Update: A Report From the American Heart Association Statistics Committee and Stroke Statistics Subcommittee. *Circulation*. 2009; 119:e21–181. [PubMed: 19075105]
- Xu B, Doughman Y, Turakhia M, Jiang W, Landsettle CE, Agani FH, Semenza GL, Watanabe M, Yang Y-C. Partial rescue of defects in *Cited2*-deficient embryos by HIF-1[alpha] heterozygosity. *Developmental Biology*. 2007; 301:130–140. [PubMed: 17022961]
- Yashiro K, Shiratori H, Hamada H. Haemodynamics determined by a genetic programme govern asymmetric development of the aortic arch. *Nature*. 2007; 450:285–288. [PubMed: 17994097]

Bullet Points

- Doppler OCT captures embryo hemodynamics
- Rapid and sensitive screening for functional phenotypes
- Heart function reflected in vitelline artery function
- Hypoxia causes rapid hemodynamic changes

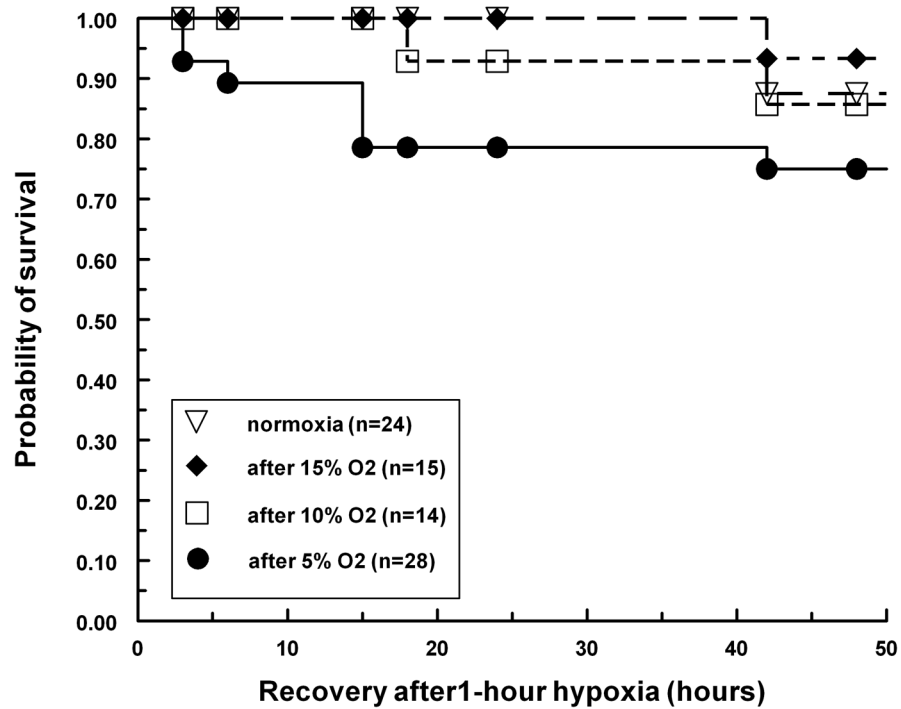


Figure 1. Survival of quail embryos post hypoxic exposure. The quail embryos (stage 17) were exposed to different degrees of hypoxia for one hour. Normal oxygen (21%) was restored at the end of the hypoxic exposure period, represented in the figure as 0 hours. Embryos were cultured for another 48-hour period, and the numbers of surviving embryos were plotted as a percentage at different time points.

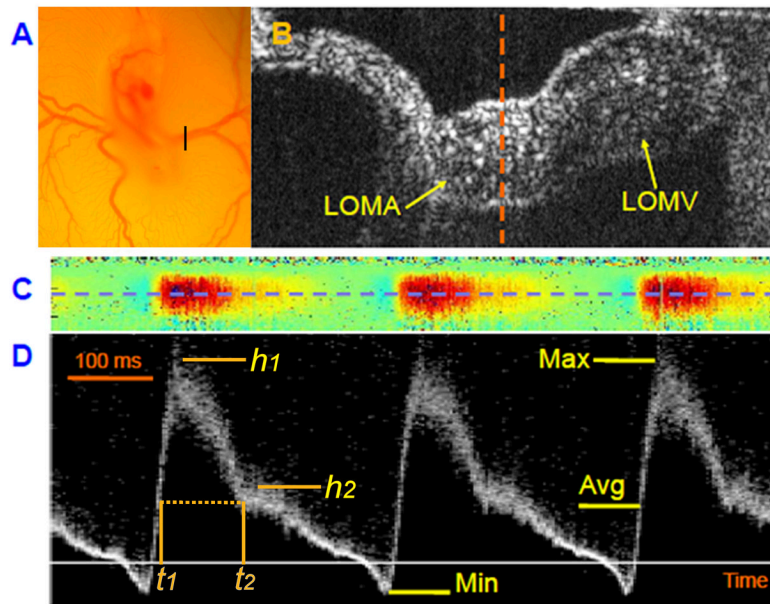


Figure 2. Doppler OCT can provide high resolution pulsed Doppler waveforms at the position of the vitelline artery for hemodynamic measurements. (1A), Microscopic view of a stage 17 quail embryo connected to the extraembryonic vasculature spreading over the yolk in an ex ovo shell-less culture. The black bar indicates the location of the vitelline vessels that was scanned for OCT imaging. (1B). B-scan OCT image of the vitelline vessel. LOMA - left omphalomesenteric artery; LOMV - left omphalomesenteric vein. (1C). Colored Doppler image at the midline of LOMA (dashed line in Figure 1B). The red color indicates forward blood flow, and the blue color indicates retrograde blood flow. (1D). Pulsed Doppler images at the center of LOMA (blue dashed line in Figure 1C). The magnitude of the signal indicates relative flow velocity with positive values representing forward blood flows. Max – maximal flow, Min – minimal flow (or maximal retrograde flow), and Avg – timed-average flow.

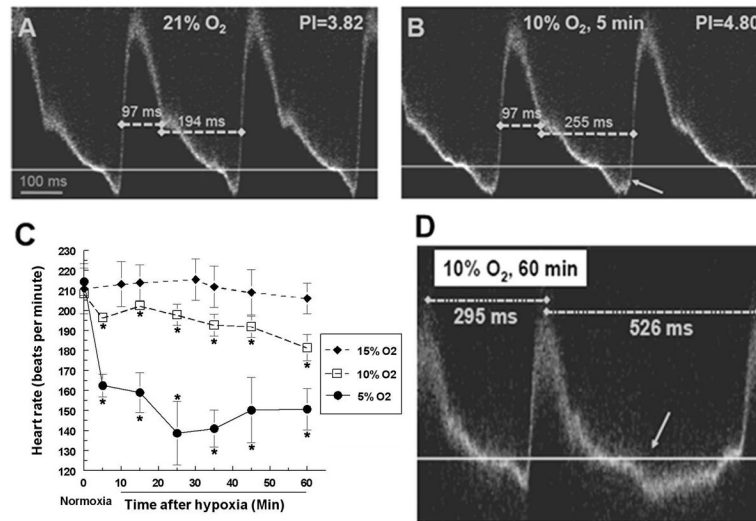


Figure 3. Changes in hemodynamic parameters, bradycardia and missing contractions were observed under hypoxic exposure. (A and B). Pulsed Doppler images of a stage 17 quail embryo before and after exposure to 10% oxygen for 5 minutes. Arrow in (B) indicates increased retrograde blood flow. (C). Embryo heart rate under different degrees of hypoxia for one hour. Numbers were averaged from 6 individual embryos in each group, and plotted as averages and standard errors (indicated by the error bars). (D). Pulsed Doppler image from a stage 17 quail embryo exposed to 10% oxygen for 1 hour. Arrow indicates a missing contraction with increased retrograde blood flow during the missing beat. Dotted lines indicate time intervals between consecutive heart beats.

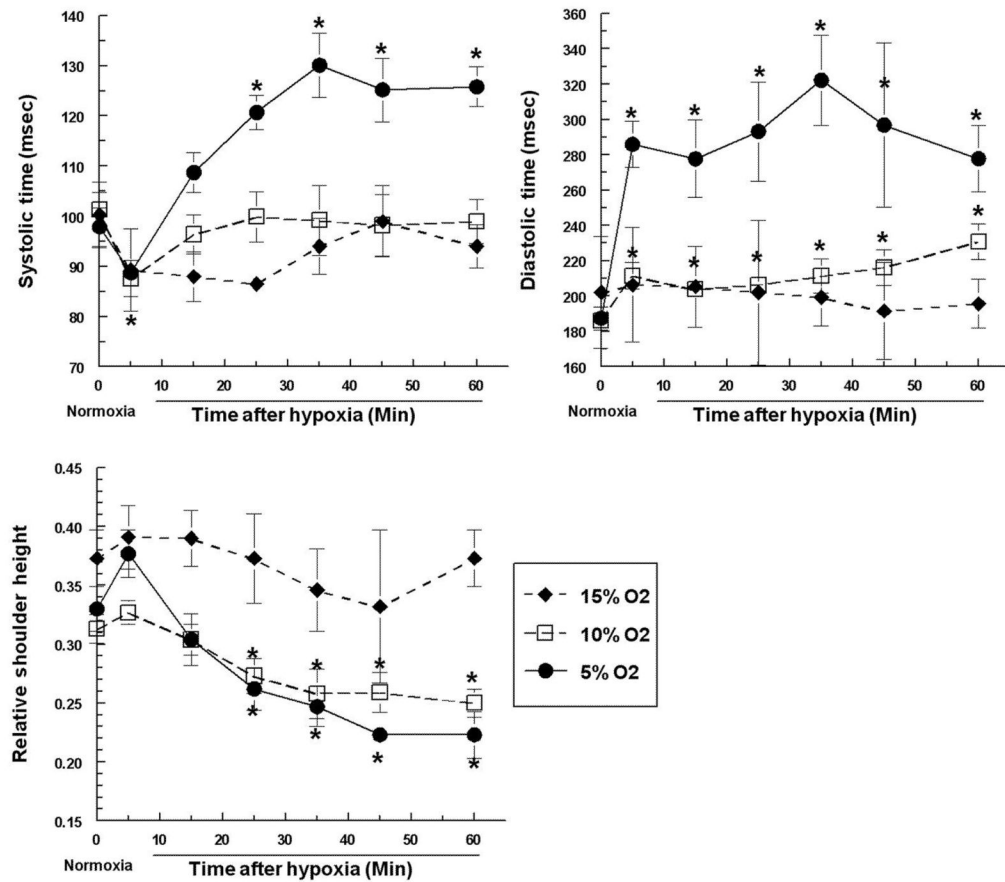


Figure 4.

Hypoxic exposure alters the systolic time, the diastolic time, and the relative shoulder height. Quail embryos were exposed to various degrees of hypoxia for 1 hour, and systolic and diastolic time was measured based on the pulsed Doppler images taken from LOMA. Relative shoulder height is defined as the ratio of the secondary peak velocity to the primary peak velocity. All numbers are averaged from 6 independent observations, and plotted as averages and standard errors. Asterisks indicate that values were statistically different from controls (prior to the hypoxic exposure) with a p-value less than 0.05.